# 3D Cycle-Consistent Adversarial Network for Designing Dental Implant Crown

Georgi Kostadinov[1(✉)] and Aleksandar Naydenov[2]

[1] New Bulgarian University, 21 Montevideo Street, 1618 Sofia, Bulgaria
grgkostadinov@gmail.com

[2] Faculty of Dental Medicine, Medical University of Sofia, 1 Georgi Sofiyski Street, 1431 Sofia, Bulgaria

**Abstract.** In this paper, we present a novel approach for designing screw retained crown over dental implant using a 3D Generative Adversarial Network (GAN), specifically 3D CycleGAN. The adversarial network was trained and validated on 3D intraoral scans from 150 patients which were adjusted for the study with ExoCad and then voxelized to a resolution of 64 × 64 × 64. Our results show an average Intersection over Union (IoU) of 75% and a mean Hausdorff distance of 1.0555 mm. This suggests a strong correlation between the generated crowns and manually designed ones, ensuring both functional and aesthetic suitability. Additionally, we generated visualizations and Hausdorff distance heatmaps to assess the alignment and deviations of the generated prostheses. The proposed approach overcomes the limitations of existing methods by fully incorporating the specific morphology of natural dental crown in the prosthesis design, resulting in crowns that are anatomically and functionally suitable for practical applications but designed without human intervention. Future enhancements include expanding the dataset with a higher variability of dental structures and increasing the input resolution of the proposed 3D CycleGAN network. Overall, our findings highlight the potential of machine learning to significantly improve the quality and efficiency of dental prosthesis design.

**Keywords:** 3D Generative Adversarial Network · Dental Prostheses · AI in Dentistry · 3D CycleGAN · Voxelization · Restorative Dentistry · Dental Crown Design · Automated Dental Design · Intersection over Union · Hausdorff Distance

## 1 Introduction

### 1.1 Background

Technological advancements have completely transformed the healthcare sector. Most notably, artificial intelligence in dental medicine has greatly improved diagnostics, treatment planning quality as well as general patient care outcomes. For instance, devices that feature Artificial Intelligence (AI) technology can enable real-time monitoring of


T. Zlateva and G. Tuparov (Eds.): CSECS 2024, LNICST 609, pp. 183–200, 2025.
https://doi.org/10.1007/978-3-031-84312-9_13

an individual's oral hygiene, thereby allowing for personalized oral health recommendations [1]. In other dental disciplines, AI is also used to make the predictive models and simulations to provide a patient-centric and, at the same time, personalized dental care [2].

The role of AI extends beyond improving diagnostics and dental care. Another cornerstone of restorative dentistry is the design of dental prostheses. It is essential to design prostheses with high precision to ensure that these artificial structures are suitable from both an anatomical and functional standpoint. The use of AI to automate the designing process ensures fewer human errors will be introduced in the 3D modelling process, leading to improved overall quality of the prostheses. At the same time, the role of human workers in creating dental implant prostheses is dramatically reduced, which means that it takes less time and costs to manufacture them [3].

This transformative potential of AI in healthcare is particularly evident with the application of 3D Generative Adversarial Networks (GANs) [4]. GANs are a class of machine learning algorithms designed by pitting two neural networks against each other: a generative network that generates new data and a discriminative network that evaluates whether this new data is generated (fake) or part of a target domain (real). Through this adversarial process, the generative network learns to produce more accurate outputs, that better represent the distribution of the target domain. A 3D GAN extends this concept into the context of three-dimensional data, enabling the generation of 3D models that can be used for creating detailed and accurate dental prostheses. This approach promises to improve dental prosthesis design, making it not only more effective but also more economical and efficient [5].

### 1.2 Literature Overview

The literature on the use of artificial intelligence in dental prosthesis design, specifically with Generative Adversarial Networks (GANs), suggests a promising direction in restorative dentistry. The studies range from methodologies for tooth segmentation using GANs [6] to the reconstruction of 3D oral structures from 2D panoramic X-rays [7], presenting a significant step forward in digital dental solutions.

In [8], a two-stage GAN designed to address the complex morphology of the occlusal surface of teeth has been presented. This study demonstrates that AI can generate dental prostheses with accurate anatomical morphology and higher clinical applicability. The proposed model outperformed other deep learning methods in reconstructing functional occlusal surfaces using a real-world patient database.

Another study [9] focused on the use of a 3-dimensional convolutional neural network (3D-CNN) to generate partial dental crowns (PDCs). This research considered the effectiveness of different scanners in capturing data for the 3D-CNN, eventually selecting intraoral scans for their superior volumetric detail. The study highlighted the ability of 3D-CNN to predict and generate PDC prostheses in CAD for restorative dentistry, marking a significant advancement in the field.

Furthermore, [10] explores a fully automatic approach that leverages natural spatial profiles between opposing teeth, which are often difficult for human technicians to account for but crucial for proper functionality. This research positions GANs as a tool that can surpass human expertise by learning from large datasets of human-designed crowns and natural fitting constraints.

In [11], Chau et al. explored the effectiveness of a novel AI system in designing biomimetic single-molar dental prostheses. The study investigated the morphology of AI-designed teeth compared to natural teeth, utilizing a Generative Adversarial Network (GAN) for the design process. Using 169 casts from healthy participants, 159 were used for GAN training, and 10 for validation. The AI system generated teeth, which were then superimposed onto the original teeth to measure morphological differences using mean Hausdorff distance and Intersection-over-Union for accuracy.

The results indicated mean Hausdorff distances ranging from 0.441 to 0.752 mm, with an Intersection-over-Union of 60%, demonstrating that the AI system could potentially automate the design of biomimetic prostheses with high accuracy. The study concludes that with further algorithm optimization and training, AI could significantly enhance the accuracy and efficiency of dental prosthesis design, suggesting a promising direction for future research and application in restorative dentistry and prosthodontics. This study is the closest related work to our research, providing a foundational comparison for our proposed methodology.

All these studies contribute to the body of knowledge, illustrating the feasibility of employing advanced AI techniques for dental prosthetic design. However, they often focus on creating crowns on a flat surface of the mold or lack the integration of the prosthesis with the unique contours of an abutment.

Considering this, our proposed methodology introduces the use of a CycleGAN [12] modified to work on 3D data that generate a crown design directly on top of the implant abutment. This novel approach aims to bridge the gap in current research by considering the full morphology of the underlying structures, thereby enhancing the practical application of the generated dental implant prosthesis.

## 2 Materials and Methods

### 2.1 Data Collection

For the purposes of our study, we conducted a comprehensive data collection process with a cohort of 150 patients. The site of the study and data collection was the Faculty of Dental Medicine at the Medical University of Sofia. Each patient's dental anatomy was digitized using intraoral scanners, iTero Element 2 plus and iTero Element 5d, specifically designed for high-precision dental imaging. These scans provided us with detailed 3D representations of the patients' dentition, essential for the subsequent stages of our research.

To process the collected data, we utilized the specialized dental software ExoCad, which allowed us to manage and manipulate the scan files effectively. We focused on tooth number 36 on the lower jaw as the focal point of our current study. For each scan of patients, we performed virtual extraction of the tooth, and a digital analog of a screw-retained titanium base abutment (GM Neodent) was placed at the site of the missing tooth. A full-coverage screw-retained crown was then digitally modeled on this abutment by trained specialist. Digital impressions of the dentition, including the lower jaw, upper jaw, and occlusion, were saved in STL file format. The STL files prepared included:

1. Upper jaw alone.
2. Lower jaw with the placed abutment, without crown.
3. Lower jaw with the placed abutment and crown.
4. Upper and lower jaw in occlusion with the placed abutment in the lower jaw, without crown.
5. Upper and lower jaw fixed in bite with the placed abutment in the lower jaw with crown.

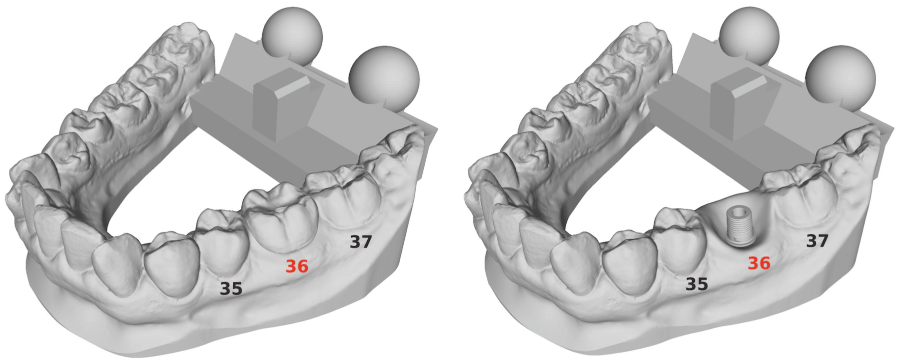


**Fig. 1.** 3D visualizations of the scanned lower jaw. Left image is with the crown designed over the abutment #36. Right image is without the crown with the abutment exposed.

Although the 3D data of the upper jaw was also collected, it was not incorporated into this phase of the research. Our data comprised pairs of STL files of the lower jaws for each patient, one with the crown designed over the abutment number 36 and the other without the crown, revealing the underlying structures of the abutment, as shown in Fig. 1.

To ensure that the generative model could learn to design the crown in proper alignment with the abutment, both files within each pair included these supporting structures. Before initiating the machine learning phase, the data was normalized and projected onto a consistent axis, standardizing the orientation and scale across all scan pairs. Subsequently, each STL file was transformed into a 512 × 512 × 512 matrix composed of binary voxel values, where ‘1’ denoted the presence of the lower jaw structure and ‘0’ indicated empty space. The voxelization process was implemented using Python and the linear algebra library Numpy.

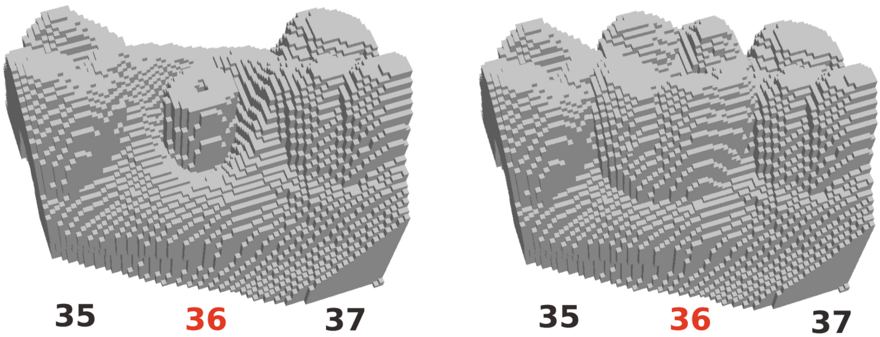


**Fig. 2.** The voxel sections used for training the GAN system. The left voxel section is without the crown and is used as the GAN source domain, the right image is with the crown design over abutment #36 and is used for the GAN target domain.

For the training of our AI model, we isolated the region encompassing implant treated place 36. We identified its precise location through the centroid of the delta computed from the voxel matrices of scans with and without the crown. This identification allowed us to extract a focused voxel section from the matrices, which included the design over the abutment of 36 and parts of its immediate neighbors, teeth numbers 35 and 37 as seen in Fig. 2. The inclusion of these adjacent teeth was essential to ensure that the generated crown would harmonize with them.

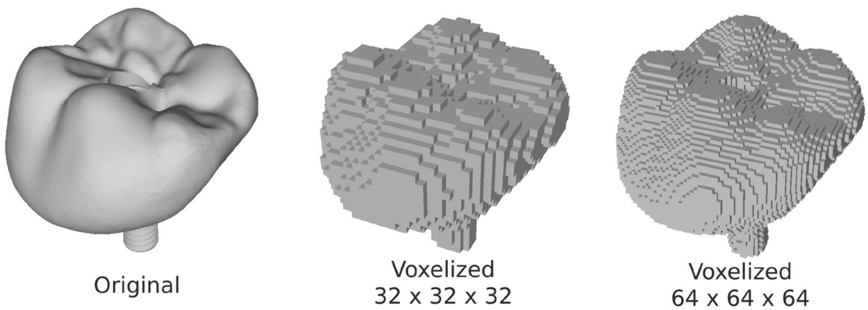


**Fig. 3.** Comparison of different voxel resolutions with the original 3D visualization of a crown with abutment. The 64 cubic resolution leads to better overall level of detail of the crown and abutment structures.

The voxel section was then scaled up to a voxel matrix of size $64 \times 64 \times 64$ as the input data size of the 3D GAN algorithm. The size of 64 cubic voxels was determined considering the memory limitations of the training hardware and after empirical evaluation and visual inspection on the level of the detail that each cubic size provided. Comparing it to 32 cubic voxels in Fig. 3, the structure of the crown is simply lacking the necessary detail for the level of quality that would be expected for a dental implant prothesis [5].

The dataset was then divided, allocating 140 samples for the training set, with the remaining 10 samples reserved for validation purposes. This split provide the GAN with a robust enough learning dataset while retaining a separate subset for performance assessment and quality measurements.

## 2.2 GAN Model Implementation

The GAN architecture selected for the implementation of the proposed work is CycleGAN [12]. It was modified to work on 64 cubic 3D data using the PyTorch framework. The CycleGAN incorporates two neural networks known as the generator and the discriminator, all trained concurrently. In this setup, the generator networks, each with a like U-Net structure [13], map data between two distinct domains A and B, where A is the domain of the lower jaw mold with abutment, while B is the domain of the lower jaw mold with the abutment and manually created crown. This pair is visualized in Fig. 1. Meanwhile the discriminators classify the generated 3D data in domains A and B as real or fake.

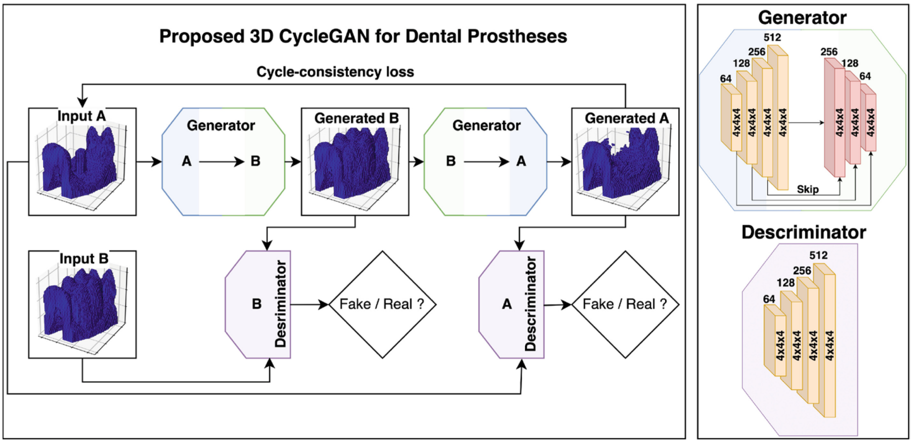


**Fig. 4.** The proposed 3D CycleGAN architecture for designing dental prostheses.

The modified 3D CycleGAN architecture, visualized on Fig. 4, includes two generators responsible for mapping data from one source domain A to another target domain B and vice versa. Generators use 3D convolutional and deconvolutional layers [14], instance normalization [15] for each convolution and deconvolution blocks, and LeakyReLU [16] activation functions to generate data close to the distribution of the target domain. There are four 3D convolutional layers of each generator network with filter sizes of $4 \times 4 \times 4$ and channel counts rising from 64 to 512. These are followed by three deconvolutional layers that reconstruct the output volume, from 256 back down to 64 channels.

Similarly to the generators, the discriminator networks have four 3D convolutional layers with filters sizes of $4 \times 4 \times 4$ and number of channels rising from 64 to 512, each followed by instance normalization layers, and LeakyReLU activations to enhance their efficiency in identifying real and fake data segments [12].

The training makes use of adversarial and cycle-consistency losses [12] to ensure that translated data retain the characteristics of the input data. The cycle consistency loss determines the deviation from the generated 3D data for domain A with that of the input data, whereas the adversarial loss determines the accuracy of both discriminators in identifying the generated data as fake. This process of training is designed to enhance the model's capability to generate convincingly real data that the discriminator cannot differentiate from actual domain data.

The models are trained for 500 epochs with Adam optimizer [17] and a learning rate of 0.0002 on hardware featuring an NVIDIA Tesla V100 graphic accelerator and an Intel Xeon processor.

### 2.3 Validation Techniques

Our validation process integrated quantitative metrics with qualitative assessments to ensure the accuracy and usability of the generated dental implant prostheses. The primary metrics used for quantitative validation are the Intersection over Union (IoU) [18] and Hausdorff distance [19].

IoU, also known as Jaccard index, is a common statistical technique in computer vision to measure the accuracy of an object detector on a particular dataset. IoU represents the ratio between the overlapping areas of the generated voxel matrix and the actual ground truth voxel matrix to their combined area, providing a robust measure of the model's precision in replicating the actual dental structures. IoU is a critical measure as it directly relates to how well the prostheses would fit within the actual dental cavity, impacting the effectiveness and comfort of the final product. On the other hand, the Hausdorff distance measures the greatest of all the distances from a point in one set to the closest point in the other set, providing a maximum bound on the discrepancy between two shapes. A lower Hausdorff distance signifies a closer match between the model-generated prosthetic design and the actual crown structure. Both metrics provide insight into the geometric accuracy [20] of the 3D models produced by our AI system.

For qualitative analysis, we generated visualizations that compared the crown voxels produced by our model against the ground truth data collected during the data acquisition phase. By doing so, we could assess the visual compatibility of the generated structures with the real manually virtual designed (wax-up) crown. Moreover, this side-by-side comparison enabled us to identify any discrepancies that might not be captured by quantitative measures alone.

To do this visual comparison, several post processing steps are applied on the output to extract the designed crown and further enhance its 3D quality. The developed pipeline is visualized in Fig. 5.

First, the generated crown is extracted using a binary exclusive or (XOR) operation [21] on the voxel data of the network input and the voxel data of the network output. The XOR operation ensures that any intersection between the input and the output will be omitted. Then, to transition from the crown's voxelized format to a usable 3D mesh model, we use the Python library Trimesh [22]. This mesh model represents the 3D surface geometry of the crown. To generate the mesh, we use the Marching Cubes

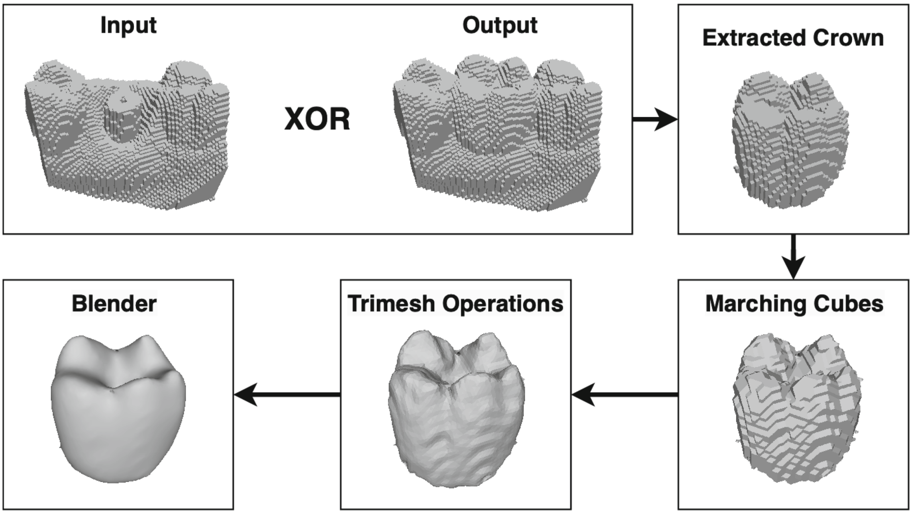


**Fig. 5.** The postprocessing pipeline that transforms the generated voxel data to a 3D model.

algorithm [23], implemented as part of the Trimesh library. Post-conversion, using the same Trimesh library, the polygon mesh undergoes a series of refining operations to enhance the quality and integrity of the 3D model. The operations applied are:

- Smooth Filter (Humphrey) [24]: This filter is used to even out the surface of the crown mesh, reducing any sharp or rough edges that resulted from the voxelization process.
- Fill Holes: This operation identifies and seales any gaps within the mesh to ensure a continuous surface, which is important for the structural integrity of the dental prosthesis.
- Fix Inversion: This procedure corrects any mesh facets whose normal vectors are incorrectly inverted, a common issue that arises during conversion from voxels to mesh.
- Fix Normals: Normal vectors of the mesh surfaces are unified to maintain a consistent orientation across the crown's surface, ensuring correct light reflection and shadow casting for accurate visualization.

Following these initial refinements, we use Blender [25], a 3D rendering software, to apply additional mesh operations. The "Deform: Smooth Vertex" function in Blender is used in achieving a smoothed final 3D mesh of the crown. This final step smooths out any remaining irregularities to ensure that the final 3D model is not only functional but also meets the high-quality standards expected in dental restorations.

## 3 Results

### 3.1 Model Performance Analysis

Tested on our validation set, which included 10 patient samples, the model achieved a mean IoU of 75%. This indicates a substantial overlap between the generated dental structures and the ground truth data, signifying a high degree of accuracy in the model's output. To calculate the Hausdorff distance between the generated and real 3D models of crowns, we used the 3D software Meshlab. The mean Hausdorff distance recorded was 1.0555 mm across the validation samples. The small value obtained reflects the precision of the model in capturing the intricate contours and edges of the dental prostheses.

The detailed performance across all validation samples is presented in Table 1, which outlines individual IoU and Hausdorff distance measures for each case. In addition to these metrics, we also examined the computational efficiency of the model. The time $t$ taken to generate each prosthetic model was recorded to evaluate the practicality of using the model in a clinical setting.

**Table 1.** Model performance results across the 10 validation samples.

| Validation Sample # | IoU | Mean Hausdorff Distance | Time $t$ (seconds) |
|---|---|---|---|
| 1 | 0.7349 | 0.9855 | 0.0241 |
| 2 | 0.8026 | 1.0325 | 0.0241 |
| 3 | 0.7832 | 0.9855 | 0.0240 |
| 4 | 0.7540 | 1.4778 | 0.0234 |
| 5 | 0.7107 | 1.2524 | 0.0231 |
| 6 | 0.6275 | 0.9755 | 0.0232 |
| 7 | 0.8382 | 0.7533 | 0.0233 |
| 8 | 0.8562 | 0.6384 | 0.0232 |
| 9 | 0.8020 | 0.7043 | 0.0225 |
| 10 | 0.6640 | 1.7495 | 0.0230 |
| Mean | 0.7573 | 1.0555 | 0.0234 |

### 3.2 Comparative Analysis

Without publicly available datasets for direct comparison, our comparative analysis relies on a methodological examination and theoretical assessments based on published results from similar studies. In [11], the authors reported that their system achieved a mean Hausdorff distance ranging from 0.441 to 0.752 mm and an Intersection-over-Union (IoU) of 60%.

While direct comparisons are limited since different datasets are used for validation and there is a clear difference in the data preparation process where we also consider the structure of the abutment, the metrics allow for a certain level of benchmarking. Our model demonstrated a Hausdorff distance between 0.638 mm and 1.749 mm, which is notably higher than the reported range from [11]. Additionally, our model achieved a mean IoU of 75%, which exceeds the reported IoU from [11], indicating a better overlap between the generated prostheses and the ground truth data.

Despite these results, it is crucial to note that variations in dataset characteristics, such as the complexity of dental structures and the specificity of the cases included, influences the outcome of the metrics.

### 3.3 Visual and Quantitate Comparisons

Visualizations for each of the 10 data samples from the validation dataset have been generated to visually analyze and compare the generated crown with the virtual wax-up provided as ground truth. The top sections of Figs. 6, 7, 8, 9, 10, 11, 12, 13, 14 and 15 visualize the input data (in blue), the generated crown (in red), and its intersection with the virtual wax-up as ground truth crown (in light blue). On the other hand, the bottom sections visualize the Hausdorff distance as a heatmap projected on the generated and postprocessed crown using the pipeline from Fig. 5. Warmer colors corelate to higher deviations (both positive or negative) between the vertex distances of the generated and the virtual wax-up crowns, whereas colder regions corelate to low or no deviations in the distances.

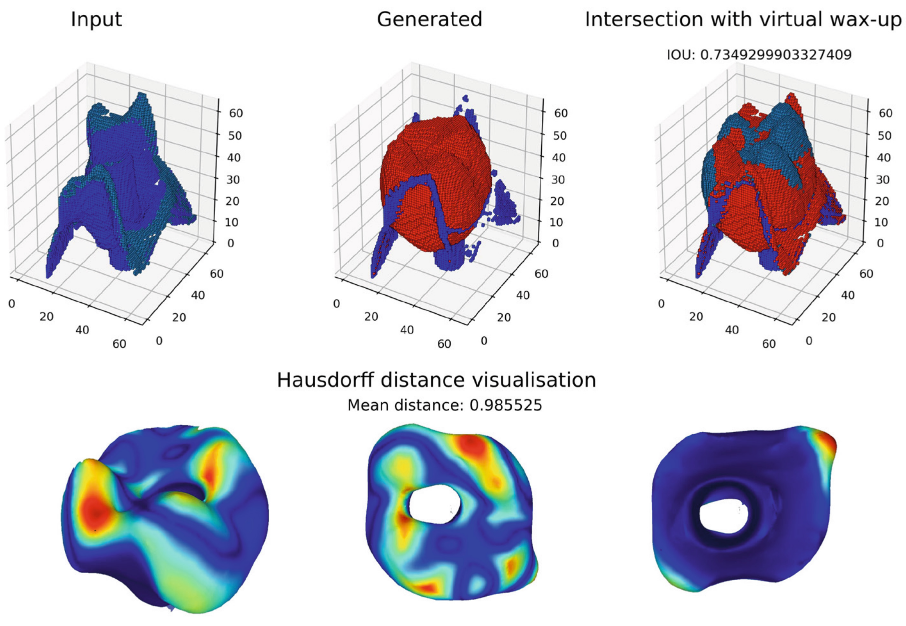


**Fig. 6.** Comparative and Hausdorff visualisations for validation sample #1.

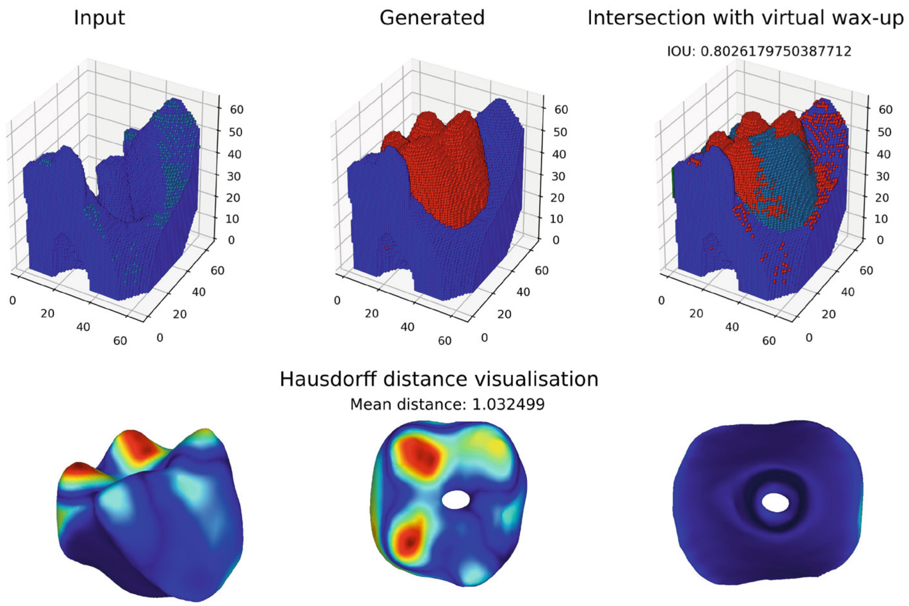


**Fig. 7.** Comparative and Hausdorff visualisations for validation sample #2.

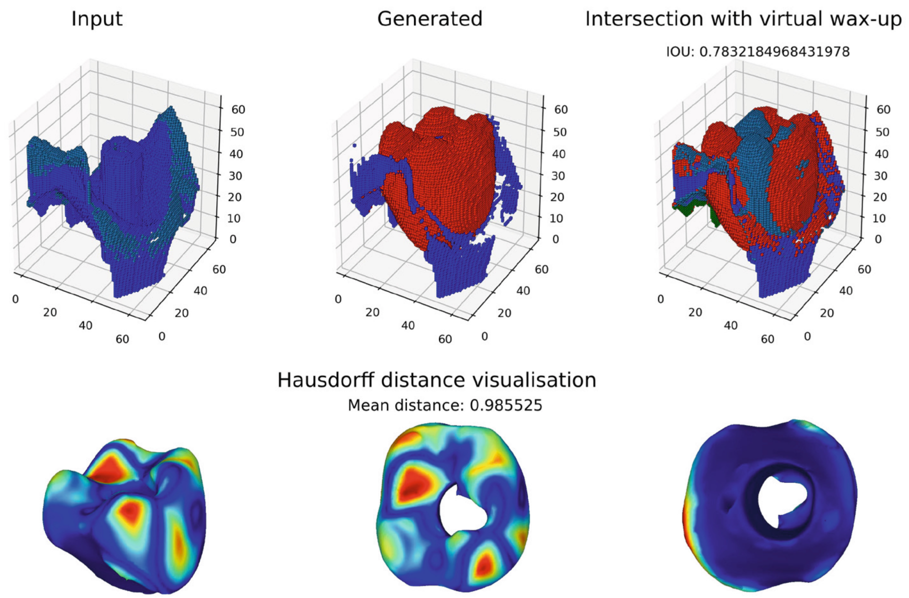


**Fig. 8.** Comparative and Hausdorff visualisations for validation sample #3.

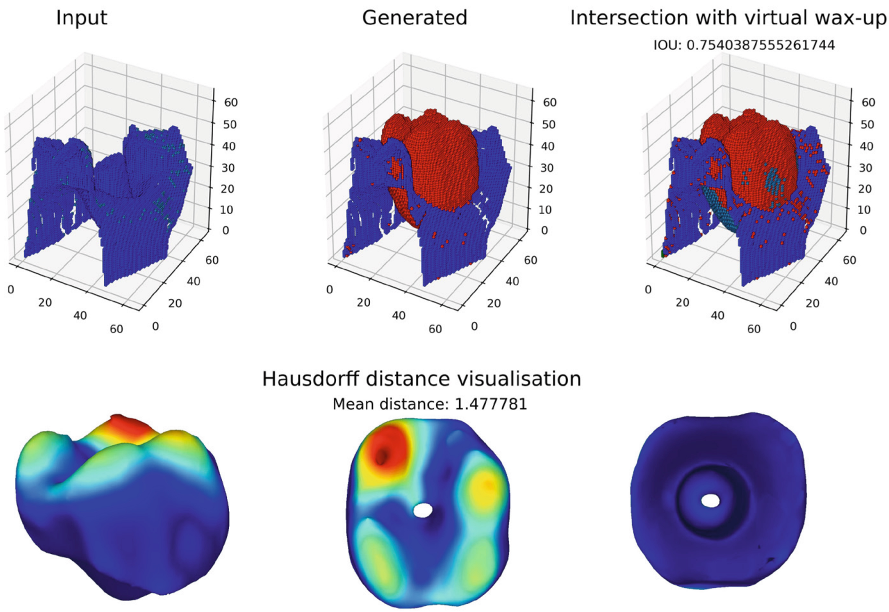


**Fig. 9.** Comparative and Hausdorff visualisations for validation sample #4.

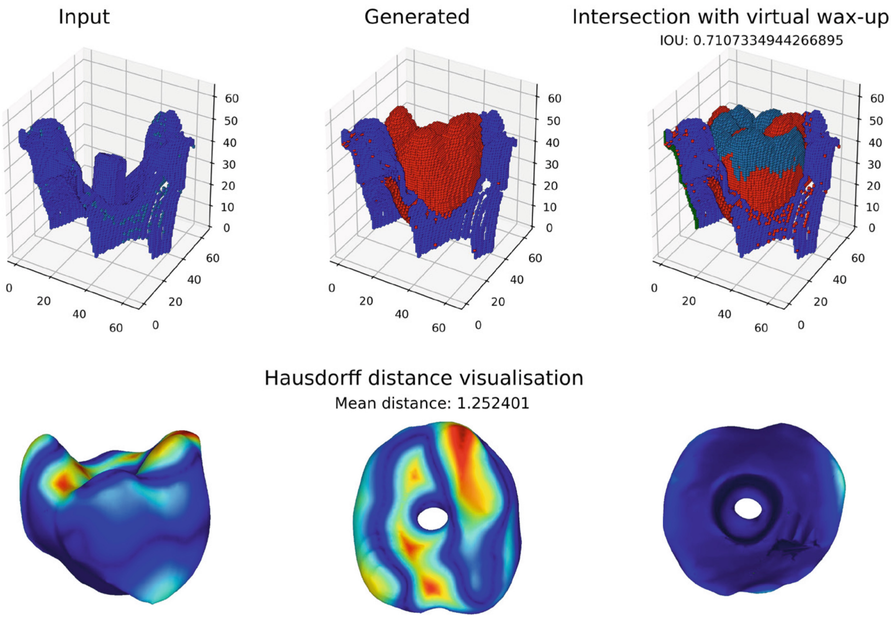


**Fig. 10.** Comparative and Hausdorff visualisations for validation sample #5.

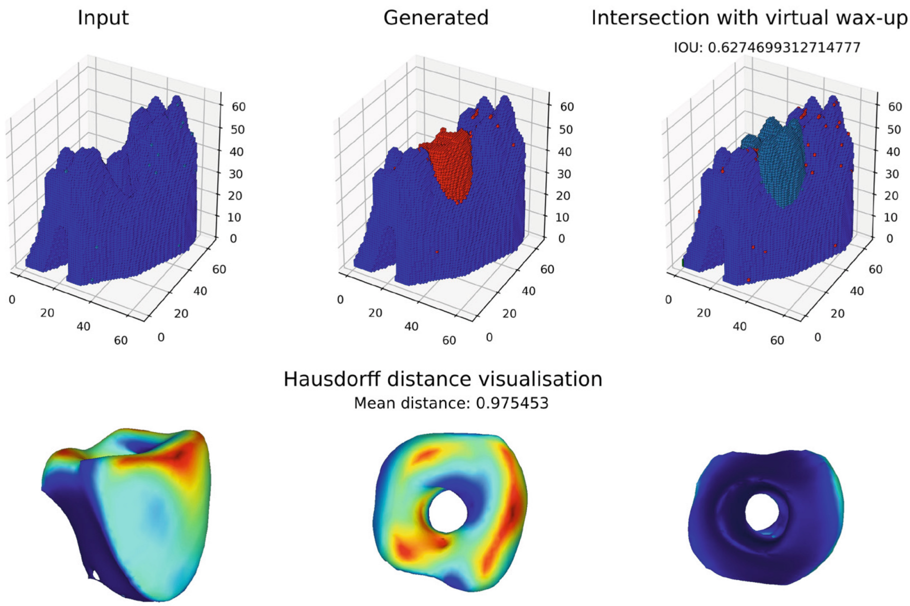


**Fig. 11.** Comparative and Hausdorff visualisations for validation sample #6.

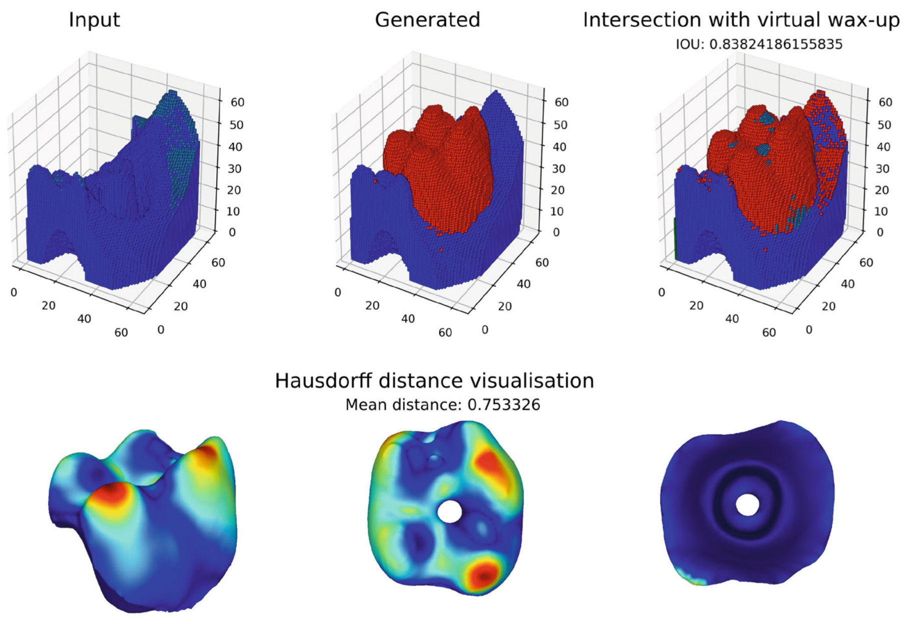


**Fig. 12.** Comparative and Hausdorff visualisations for validation sample #7.

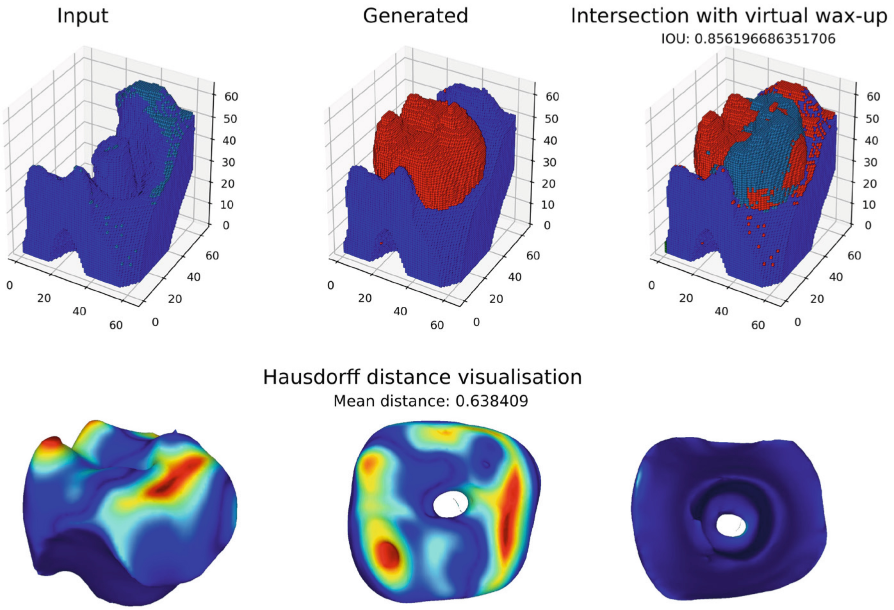


**Fig. 13.** Comparative and Hausdorff visualisations for validation sample #8.

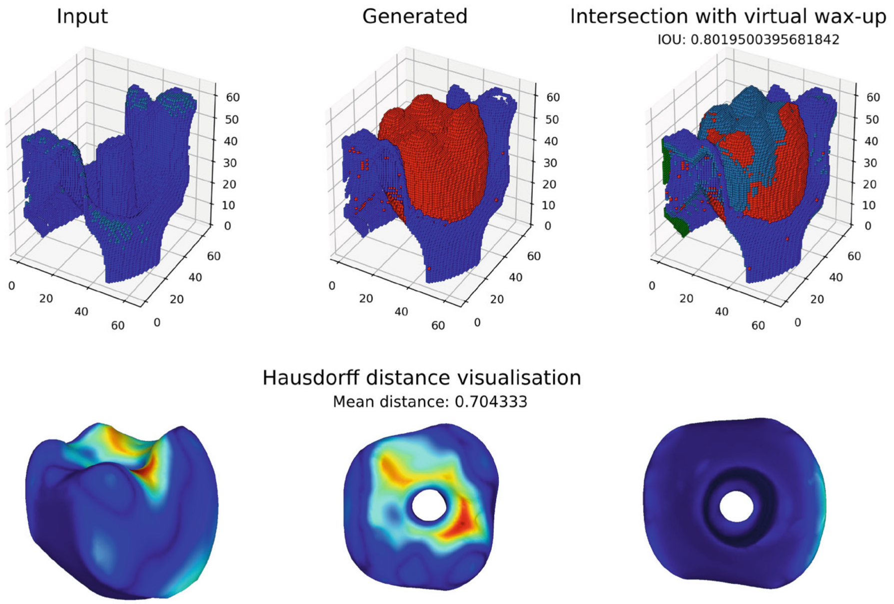


**Fig. 14.** Comparative and Hausdorff visualisations for validation sample #9.

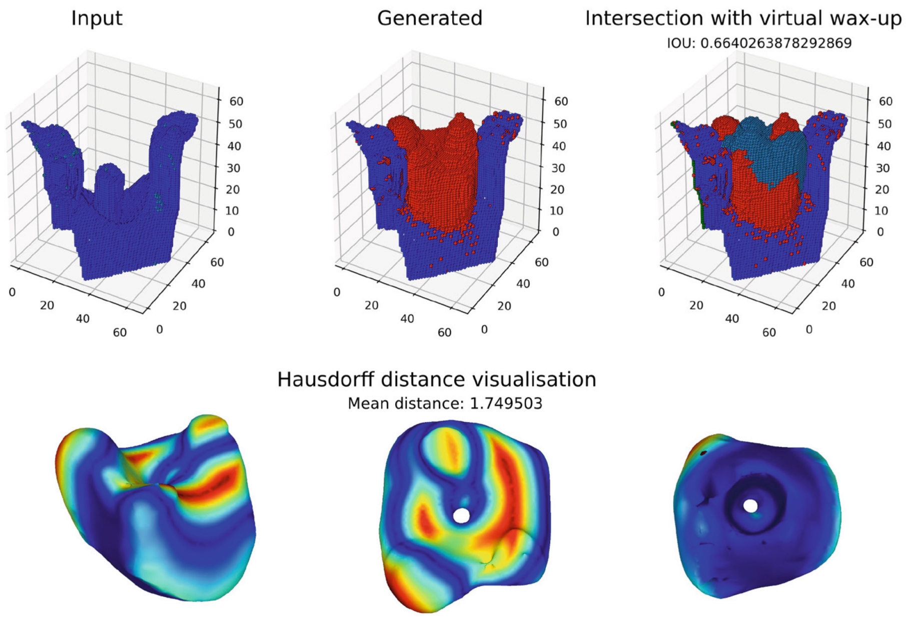


**Fig. 15.** Comparative and Hausdorff visualisations for validation sample #10.

# 4 Discussion

## 4.1 Interpretation of Results

The results of our study indicate that the application of a 3D CycleGAN for the design of dental implant prostheses is both effective and efficient. The Intersection over Union (IoU) scores, averaging 75%, suggest a strong alignment between the generated prosthetic models and the ground truth data. This high degree of overlap is indicative of the model's proficiency in replicating the intricate structures of dental implant crowns, ensuring that the prostheses are likely to correspond with high value due to the implant abutment, adjacent teeth and underlying mucosa.

The Hausdorff distance, with a mean value of 1.0555 mm, further supports the model's accuracy in capturing the geometric details of the teeth. This metric is particularly important as it measures the maximum deviation between the generated model and the actual crown structure, thus providing a comprehensive assessment of the model's precision. The relatively low Hausdorff distance demonstrates that the generated prostheses are closely aligned with the pre virtual wax-up structures, which is crucial for both aesthetic and functional outcomes in restorative dentistry.

Additionally, the time efficiency of the model, averaging around 0.0234 s per prosthetic generation, highlights the practical applicability of our approach in clinical settings. This rapid generation time is beneficial for dental practitioners, allowing for quick process of design and production of customized prostheses, thereby enhancing patient experience, and reducing the overall time required for dental restoration procedures.

### 4.2 Limitations

Despite the promising results, there are several limitations to our study. One significant limitation is the reliance on a specific dataset comprising data of implant crown design for 36. While this provided a controlled environment for model training and validation, it may limit the generalizability of our findings to other teeth and broader dental implant structures. Future studies should include a more diverse range of dental scans, including such that incorporate both the lower and upper jaws, to enhance the model's applicability across different dental scenarios.

Another limitation is the voxel resolution used in the model. Although a $64 \times 64 \times 64$ voxel grid was selected based on hardware constraints and empirical evaluations, higher resolutions could potentially improve the detail and accuracy of the generated prostheses. However, this would require more advanced hardware and could increase the computational cost, which needs to be balanced against the benefits of higher resolution outputs.

The qualitative assessment, while useful, is subjective and may not capture all discrepancies between the generated and actual dental structures. Incorporating more objective measures, automated evaluation tools, or even real-life trials of the generated prostheses could provide a more comprehensive assessment of the model's performance.

### 4.3 Future Directions

Future research should focus on expanding the training dataset to include a wider variety of dental structures and conditions. This would help in developing a more versatile model capable of generating accurate prostheses for different site of implantations and varying degrees of dental implant structures. Additionally, exploring higher voxel resolutions and advanced hardware solutions could enhance the detail and accuracy of the generated models.

Integrating other machine learning techniques, such as reinforcement learning [26] or advanced neural network architectures such as vision transformers [27] or diffusion models [28], could further improve the model's performance. These approaches could provide more robust learning algorithms that adapt better to the nuances of dental implant structures.

Moreover, collaboration with dental professionals to incorporate clinical feedback into the model's development process could lead to more clinically relevant outcomes. This user-centered approach would ensure that the generated prostheses not only meet technical specifications but also align with practical clinical needs and patient expectations.

## 5 Conclusions

In conclusion, this study demonstrates the potential of 3D CycleGANs in assisting the design of dental implant prostheses. The model's high IoU and low Hausdorff distance indicate that it can generate prostheses with high accuracy and detail, closely resembling to the pre virtual wax-up structures. The rapid generation time further underscores its practicality for clinical use, promising significant improvements in the efficiency and effectiveness of dental restoration procedures.

However, to fully realize the potential of this technology, future research should address the current limitations by expanding the dataset diversity, exploring higher resolutions, and integrating more advanced machine learning techniques. Collaborative efforts with dental professionals will be essential to refine the model and ensure its clinical relevance and applicability.

By addressing these areas, we can enhance the quality and accessibility of dental prostheses, ultimately improving patient outcomes and advancing the field of restorative dentistry.

**Acknowledgements.** This work was supported by the Central Fund for Strategic Development at New Bulgarian University, Sofia. We also thank the Faculty of Dental Medicine at the Medical University of Sofia for providing the essential tools, premises, and software needed for data collection, supported by project "Д-130/29.06.2024" under the "ГРАНТ 2024 за ФИНАНСИРАНЕ НА НАУЧНИ ИЗСЛЕДВАНИЯ" program. Their invaluable contributions were crucial to the research documented in this paper.

## References

1. Dwivedi, Y.K., et al.: Artificial Intelligence (AI): multidisciplinary perspectives on emerging challenges, opportunities, and agenda for research, practice and policy. Int. J. Inf. Manage. **57**, 101994 (2021)
2. Fruehwirt, W., Duckworth, P.: Towards better healthcare: What could and should be automated? Technol. Forecast. Soc. Chang. **172**, 120967 (2021)
3. Baroudi, K., Ibraheem, S.N.: Assessment of chair-side computer-aided design and computer-aided manufacturing restorations: a review of the literature. J. Int. Oral Health JIOH **7**(4), 96 (2015)
4. Goodfellow, I., et al.: Generative adversarial nets. Adv. Neural Inf. Process. Syst. **27** (2014)
5. Marta, R.L., et al.: Artificial intelligence models for tooth-supported fixed and removable prosthodontics: a systematic review. J. Prosthet. Dent. **129**(2), 276–292 (2023)
6. Kim, T., et al.: Tooth segmentation of 3D scan data using generative adversarial networks. Appl. Sci. **10**(2), 490 (2020)
7. Song, W., et al.: Oral-3d: Reconstructing the 3d structure of oral cavity from panoramic x-ray. In: Proceedings of the AAAI Conference on Artificial Intelligence. vol. 35, no. 1 (2021)
8. Tian, S., et al.: DCPR-GAN: dental crown prosthesis restoration using two-stage generative adversarial networks. IEEE J. Biomed. Health Inform. **26**(1), 151–160 (2021)
9. Farook, T.H., et al.: Computer-aided design and 3-dimensional artificial/convolutional neural network for digital partial dental crown synthesis and validation. Sci. Rep. **13**(1), 1561 (2023)
10. Hwang, J.J., et al.: Learning beyond human expertise with generative models for dental restorations. arXiv preprint arXiv:1804.00064 (2018)
11. Chau, R.C.W., et al.: Accuracy of artificial intelligence-designed single-molar dental prostheses: a feasibility study. J. Prosthet. Dent. (2023)
12. Zhu, J.-Y., et al.: Unpaired image-to-image translation using cycle-consistent adversarial networks. In: Proceedings of the IEEE International Conference on Computer Vision (2017)
13. Ronneberger, O., Fischer, P., Brox, T.: U-Net: convolutional networks for biomedical image segmentation. In: Navab, N., Hornegger, J., Wells, W., Frangi, A. (eds.) Medical Image Computing and Computer-Assisted Intervention – MICCAI 2015. MICCAI 2015. Lecture Notes in Computer Science(), vol. 9351. Springer, Cham (2015). https://doi.org/10.1007/978-3-319-24574-4_28

14. Maturana, D., Scherer, S.: Voxnet: a 3d convolutional neural network for real-time object recognition. In: 2015 IEEE/RSJ International Conference on Intelligent Robots and Systems (IROS). IEEE (2015)
15. Dmitry, U., Vedaldi, A., Lempitsky, V.: Instance normalization: The missing ingredient for fast stylization. arXiv preprint arXiv:1607.08022 (2016)
16. Xu, B., et al.: Empirical evaluation of rectified activations in convolutional network. arXiv preprint arXiv:1505.00853 (2015)
17. Kingma, D.P., Ba, J.: Adam: A method for stochastic optimization. arXiv preprint arXiv:1412.6980 (2014)
18. Rezatofighi, H., et al.: Generalized intersection over union: a metric and a loss for bounding box regression. In: Proceedings of the IEEE/CVF Conference on Computer Vision and Pattern Recognition (2019)
19. Felix, H.: Grundzüge der mengenlehre, vol. 7. von Veit (1914)
20. Taha, A.A., Hanbury, A.: Metrics for evaluating 3D medical image segmentation: analysis, selection, and tool. BMC Med. Imaging **15**, 1–28 (2015)
21. Bocheński, J.M., Bird, O.: A Precis of Mathematical Logic. Reidel, Dordrecht (1959)
22. Michael, D.H.: trimesh. Python library (2019)
23. Lorensen, W.E., Cline, H.E.: Marching cubes: a high resolution 3D surface construction algorithm. In: Seminal Graphics: Pioneering Efforts that Shaped the Field, pp. 347–353 (1998)
24. Vollmer, J., Mencl, R., Mueller, H.: Improved laplacian smoothing of noisy surface meshes. Comput. Graph. Forum. **18**(3). Oxford, UK and Boston, USA: Blackwell Publishers Ltd (1999)
25. Blender, O.: Blender—A 3D modelling and rendering package. Retrieved. represents the sequence of Constructs1 to 4 (2018)
26. Kaelbling, L.P., Littman, M.L., Moore, A.W.: Reinforcement learning: a survey. J. Artif. Intell. Res. **4**, 237–285 (1996)
27. Khan, S., et al.: Transformers in vision: a survey. ACM Comput. Surv. (CSUR) **54**(10s), 1–41 (2022)
28. Croitoru, F.A., et al.: Diffusion models in vision: a survey. IEEE Trans. Pattern Analy. Mach. Intell. (2023)